Dual-Responsive Magnetic Core-Shell Nanoparticles for Non-Viral Gene Delivery and Cell Separation

Alexander P. Majewski[1], Anja Schallon[2], Valérie Jérôme[2], Ruth Freitag[2], Axel H. E. Müller[1], Holger Schmalz[1]

[1]Makromolekulare Chemie II and [2]Bioprozesstechnik, Universität Bayreuth, 95440 Bayreuth, Germany

Introduction

There exist two main approaches for the functionalization of nanoparticles (NPs) with polymer chains fixed on the NPs' surface. The "grafting-to" method is performed by utilizing polymers bearing suitable functional end groups (anchor groups), which are able to bind to the surface of the particle. Alternatively, the "grafting-from" approach can be used to obtain core-shell nanoparticles. In this case, the initiating moiety is immobilized on the nanoparticle surface and the polymerization takes place directly from the surface.[1,2]

We present the synthesis of core-shell NPs *via* the grafting-from approach utilizing a dopamine based ATRP initiator. Dopamine is considered to be a robust anchor for iron oxide surfaces in aqueous media. Grafting of 2-(dimethylamino)ethyl methacrylate (DMAEMA) via surface-initiated ATRP yielded dual responsive core-shell NPs being responsive to temperature and pH. Due to the great potential of cationic polymers for non-viral gene delivery the hybrid material was further investigated related to biotechnical applications. The cytotoxicity and the efficiency as transfection reagent were studied under standard conditions and compared to the "gold standard" poly(ethylene imine), PEI.

Experimental

Materials. Copper(I) chloride was purified according to literature[3] and the monomer 2-(dimethylamino)ethyl methacrylate (DMAEMA) was destabilized by passing through a basic aluminum oxide column. The synthesis of the dopamine based ATRP initiator 2-bromo-N-[2-(3,4-dihydroxyphenyl)-ethyl]-isobutyrylamide (2-bromoisobutyryl dopamide, BIBDA) and oleic acid stabilized maghemite (γ-Fe_2O_3) nanoparticles was performed as described elsewhere.[4,5] The maghemite nanoparticles were functionalized with the dopamine based ATRP initiator via ligand exchange in THF. Finally, the hybrid core-shell nanoparticles were prepared by surface-initiated ATRP of DMAEMA in anisole. All other materials were used as received.

Plasmid DNA was prepared by using the EndoFree Plasmid Kit from Qiagen. Plasmid pH2B-EGFP (5.1 kb) encoding the nuclei localized EGFP (enhanced green fluorescent protein) driven by the cytomegalovirus immediate early promoter was used in all transfection experiments. The plasmid was amplified in *E. coli DH5 alpha* strain in LB medium to sufficient quantities by using standard molecular biology techniques, including harvesting and purification *via* Qiagen's Giga-Prep kits. Plasmid DNA (pDNA) concentration and quality were determined by $A_{260}/_{280}$ ratio and by agarose gel electrophoresis.

Instrumentation. The molecular weight distribution of the grafted PDMAEMA chains was determined via SEC using dimethylacetamide as eluent and applying a PDMAEMA calibration. Turbidity measurements were carried out with a Spectrosense 523 nm (Metrohm). The temperature program (1 K/min) was run by a thermostat. TGA was performed using a Mettler Toledo TGA/SDTA 85. The stability of the NPs was investigated by Asymmetric flow field-flow fractionation (AF-FFF, Wyatt). Magnetization curves were recorded using a Lake Shore vibrating sample magnetometer. The functionalization of the dopamine initiator was examined by FT-IR. The relative expression of EGFP fluorescence of 1 x 10^4 cells was quantified *via* flow cytometry (Beckman Coulter). The cells separated via a magnet were analyzed by epifluorescence microscopy.

Results and Discussion

Magnetic hybrid nanoparticles (γ-Fe_2O_3@$(PDMAEMA_{590})_{46}$) bearing 46 $PDMAEMA_{590}$ arms (subscript denotes the number-average degree of polymerization) were synthesized via the grafting-from approach, utilizing a dopamine-functionalized ATRP initiator (2-bromoisobutyryl dopamide, BIBDA). The cloud point of PDMAEMA depends on pH leading to dual-responsive behavior (**Scheme 1**).

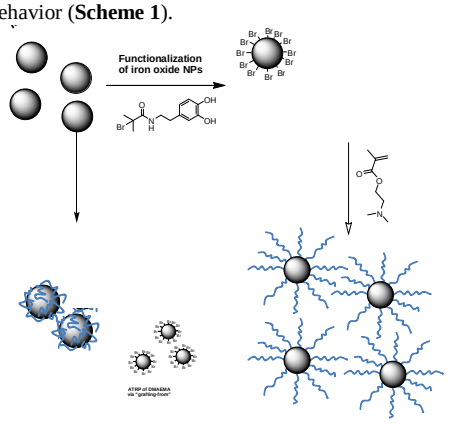

Scheme 1. Synthesis of dual-responsive maghemite nanoparticles.

The comparison of the FT-IR spectra of the ATRP initiator functionalized NPs (γ-Fe_2O_3@BIBDA) with the spectra of oleic acid stabilized NPs (γ-Fe_2O_3@Oleic acid), pure oleic acid, and pure BIBDA clearly confirms a successful functionalization (**Figure 1**). After ligand exchange with BIBDA the maghemite nanoparticles show the specific dopamine bands at 3700-3100 cm^{-1} and 1650 cm^{-1}, corresponding to hydroxyl/amide (-O-H; N-H) and amide I (C=O) bonds, respectively. However, a remaining small shoulder at 1700 cm^{-1} (carbonyl, C=O) in the IR spectrum of γ-Fe_2O_3@BIBDA indicates that the surface is still covered partially by oleic acid.

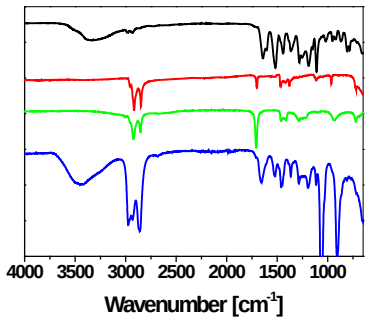

Figure 1. FT-IR spectra of pure BIBDA (black), pure oleic acid (green), oleic acid stabilized nanoparticles γ-Fe_2O_3@Oleic acid (red), and BIBDA-functionalized nanoparticles γ-Fe_2O_3@BIBDA (blue).

Further investigations to quantify the amount of BIBDA on the surface of the NPs were performed by thermogravimetric analysis (TGA). BIBDA shows a characteristic degradation step at much higher temperatures compared to oleic acid. Thus, this specific weight loss was used to calculate the weight fraction of the attached BIBDA. In addition, the bromine content was measured by ion chromatography, which in turn also allows to calculate the BIBDA content. The calculations revealed a grafting density of ca. 415 initiator molecules per particle.

The PDMAEMA grafted NPs were purified by heating above the cloud point of γ-Fe_2O_3@$(PDMAEMA_{590})_{46}$ at high pH taking advantage of the significant lower cloud point compared to the free polymer (discussed later in **Figure 2**). Asymmetric flow field-flow fractionation (AF-FFF) measurements were conducted right after purification showing only an negligible amount of non-bound polymer, which allows the determination of the initial grafting density. For an evaluation of the grafting density by TGA, the molecular weight of the grafted PDMAEMA chains was determined by cleaving the chains from the iron oxide core *via* hydrolysis with hydrochloric acid and subsequent SEC analysis, yielding M_n(PDMAEMA) = 93.000 g/mol (PDI = 1.22). From the observed weight loss in TGA a grafting density of ca. 46 PDMAEMA chains/particle (γ-Fe_2O_3@$(PDMAEMA_{590})_{46}$) was obtained.

Further AF-FFF studies were performed to investigate the long term stability of the grafted particles. For this purpose, samples were measured after

storage for different times up 140 days. Although the particles are highly stable and well dispersed in aqueous media for months a slow detachment of the grafted PDMAEMA chains was observed. The measurements revealed a continuous increase of the fraction of non-bound polymer with time. The kinetics of this process indicates a fast loss of polymer chains at the beginning, which is continuously slowing down. An equilibrium state is observed after more than 100 days.

Due to the reversible binding of the PDMAEMA chains we used freshly purified NPs bearing 53 $PDMAEMA_{590}$ arms (γ-Fe_2O_3@$(PDMAEMA)_{590})_{53}$) to investigate the dual-responsive behavior *via* turbidimetry. These results were compared with the solution properties of the cleaved-off linear $PDMAEMA_{590}$ chains and a 24-arm PDMAEMA homopolymer star ($(PDMAEMA_{240})_{24}$)[6] (**Figure 2**). Since there is a strong influence of the molecular weight on the cloud point especially at high pH,[6] the cloud point of the PDMAEMA-grafted NPs (having a ca. 50-fold higher molecular weight) is supposed to be lower than that of the corresponding cleaved-off arms. This is indeed observed. Whereas the cloud points of the hybrid star and those of the 24-arm PDMAEMA star are very close, those of the free arms are higher by about 5 K at pH 10.

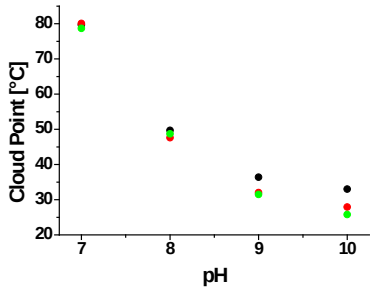

Figure 2. Cloud points in dependence on pH for 0.1 g/L solutions of cleaved $PDMAEMA_{590}$ (black), γ-Fe_2O_3@$(PDMAEMA_{590})_{53}$ (red), and a $(PDMAEMA_{240})_{24}$ star (green).[6]

The magnetization curve reveals the superparamagnetic behavior of the hybrid material caused by the iron oxide core. **Figure 3** shows the typical sigmoidal shape without hysteresis indicating that magnetic redistribution takes place via internal (Néel) relaxation. Steric and electrostatic repulsion of the PDMAEMA chains keep the particles well dispersed in solution. As a result, the hybrid nanoparticles cannot be separated by a magnet. In contrast, above the cloud point of PDMAEMA the particles start to agglomerate and thus are attracted by a magnet.

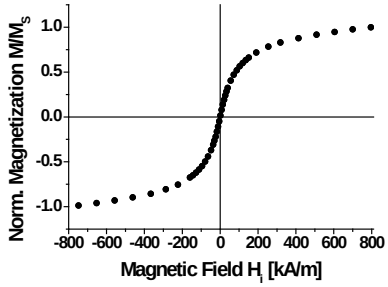

Figure 3. Normalized magnetization curve of γ-Fe_2O_3@$(PDMAEMA_{590})_{46}$.

MTT assays were performed on CHO-K1 cells to evaluate the metabolic activity of L929 cells exposed to γ-Fe_2O_3@$(PDMAEMA_{590})_{46}$ hybrid particles and PEI homopolymer under conditions mimicking transfection conditions. Under these conditions, the LD_{50} for cells treated with the polycations are 0.09 ± 0.003 mg/mL (γ-Fe_2O_3@$(PDMAEMA_{590})_{46}$) and 0.06 ± 0.004 mg/mL (PEI), respectively. Consequently, the hybrid particles exhibit a lower cytotoxicity although the molecular weight is significant higher than that of the utilized PEI.

The transfection efficiency of γ-Fe_2O_3@$(PDMAEMA_{590})_{46}$ was explored under standard conditions in CHO-K1 cells and compared to the "golden standard" PEI. Results performed by flow cytometry showed that the γ-Fe_2O_3@$(PDMAEMA_{590})_{46}$ led to a high transfection efficiency depending on the N/P ratio and performed best at N/P = 10 - 20 with averaged transfection efficiencies between 53.5 ± 12.4% and 61.4 ± 6.6%. Corresponding experiments with PEI led at most to 27.6 ± 11.2% transfected cells in accordance to data published elsewhere.[7] In all cases, the cell viability was above 75% as measured by counterstaining the dead cells with propidium iodide.

Due to the magnetic properties of the hybrid NPs cells transfected with γ-Fe_2O_3@$(PDMAEMA_{590})_{46}$/pDNA polyplexes acquire magnetic properties. For verification, CHO-K1 cells were transfected, harvested after 24 h and then incubated overnight in the vicinity of a magnet. Analysis of the cells localization by epifluorescence microscopy showed that most of the cells, transfected with γ-Fe_2O_3@$(PDMAEMA_{590})_{46}$, segregated on the wall of the cuvette facing the magnet and thus displayed magnetic properties (**Figure 4A,C,D**). By comparison, most of the cells transfected with PEI were found to sediment at the bottom of the cuvette (**Figure 4B**).

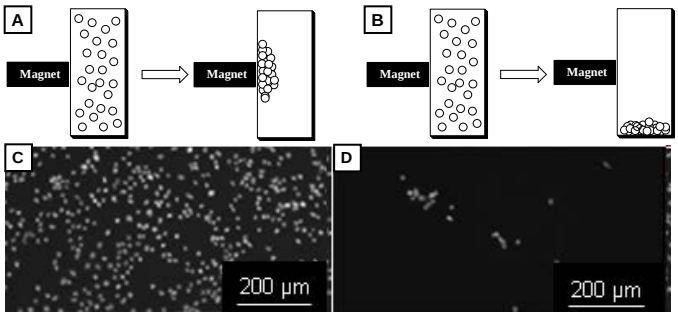

Figure 4. Separation scheme of cells transfected with polyplexes based on γ-Fe_2O_3@$(PDMAEMA_{590})_{46}$ (A) and PEI (B). Fluorescence microscopy images of the cells transfected with γ-Fe_2O_3@$(PDMAEMA_{590})_{46}$/pDNA polyplexes grown next to the magnet (C) and on the opposite site (D).

Conclusions

We demonstrated the successful synthesis of dual responsive core-shell NPs *via* the grafting-from approach utilizing a dopamine based initiator. Despite the reversible binding of the PDMAEMA chains our present approach already provides magnetic core-shell nanoparticles of sufficient solubility and stability in aqueous media over several months. Cell transfection experiments showed that γ-Fe_2O_3@$(PDMAEMA_{590})_{46}$ offers the great advantage to combine a high transfection efficiency (almost twofold higher than PEI) with a low *in vitro* cytotoxicity and should be considered as a good candidate for delivery of plasmid DNA. Moreover, taking advantage of the magnetic properties of the γ-Fe_2O_3@PDMAEMA/pDNA polyplexes, these NPs provide a tool that allows the identification/isolation of cells containing polyplexes and thus the removal of non-transfected cells.

Acknowledgements. This work was supported by the DFG priority program SPP 1259. We thank Sandrine Tea and Marietta Böhm for SEC and AF-FFF measurements and Thomas Friedrich for VSM measurements.

References

(1) Lutz, J.-F.; Stiller, S.; Hoth, A.; Kaufner, L.; Pison, U.; Cartier, R. *Biomacromolecules* **2006**, *7*, 3132.
(2) Gelbrich, T.; Feyen, M.; Schmidt, A. M. *Macromolecules* **2006**, *39*, 3469.
(3) Plamper, F. A.; Becker, H.; Lanzendörfer, M.; Patel, M.; Wittemann, A.; Ballauff, M.; Müller, A. H. E. *Macromol. Chem. Phys.* **2005**, *206*, 1813.
(4) Fan, X.; Lin, L.; Dalsin, J. L.; Messersmith, P. B. *J. Am. Chem. Soc.* **2005**, *127*, 15843.
(5) Hyeon, T.; Lee, S. S.; Park, J.; Chung, Y.; Na, H. B. *J. Am. Chem. Soc.* **2001**, *123*, 12798.
(6) Plamper, F. A.; Ruppel, M.; Schmalz, A.; Borisov, O.; Ballauff, M.; Müller, A. H. E. *Macromolecules* **2007**, *40*, 8361.
(7) Schallon, A.; Jérôme, V.; Walther, A.; Synatschke, C. V.; Müller, A. H. E.; Freitag, R. *React. Funct. Polym.* **2010**, *70*, 1.